# Active arc suppression device based on voltage-source convertor with consideration of line impedance in distribution networks

Fan, Bishuang; Ma, Haihang; Wang, Wen; Yao, Ganzhou; Li, Qikai; Zeng, Xiangjun; Guerrero, Josep M.

*Published in:*
IET Power Electronics

*DOI (link to publication from Publisher):*
10.1049/pel2.12203



*Publication date:*
2021

*Document Version*
Publisher's PDF, also known as Version of record

Received: 21 April 2021 | Revised: 12 August 2021 | Accepted: 19 September 2021

IET Power Electronics

DOI: 10.1049/pel2.12203

The Institution of Engineering and Technology WILEY

ORIGINAL RESEARCH PAPER

# Active arc suppression device based on voltage-source convertor with consideration of line impedance in distribution networks

**Bishuang Fan**[1] | **Haihang Ma**[1] | **Wen Wang**[1] | **Ganzhou Yao**[1] | **Qikai Li**[1] | **Xiangjun Zeng**[1] | **Josep M. Guerrero**[2]

[1] School of Electrical and Information Engineering, Changsha University of Science & Technology, Changsha, China

[2] Department of Energy Technology, Aalborg University, Aalborg, Denmark

**Correspondence**
Wen Wang, School of Electrical and Information Engineering, Changsha University of Science & Technology, Changsha 410114, China.
Email: wew@csust.edu.cn

**Funding information**
National Natural Science Foundation of China, Grant/Award Numbers: 51877011, 52077010; Training Program for Excellent Young Innovators of Changsha, Grant/Award Number: kq2009011

**Abstract**

In the non-effectively grounding distribution system, residual current under single-line-to-ground (SLG) fault threatens the safety of human being and power supply equipment. Active arc suppression device has been proved to be effective for SLG fault arc suppression when the line impedance is ignored. However, in practice, line impedance varies with the fault location and the load current flowing through the impedance brings about additional voltage drop, which increases the fault current and is not dealt with by the conventional methods. To achieve accurate SLG fault arc suppression with the existence of line impedance, the neutral-to-ground voltage reference for full ground-fault current compensation is firstly derived and a detection method is then proposed. The pre-fault and post-fault line currents are used to eliminate the influence of load current on the line impedance voltage drop. A dual-loop voltage and current controller is then designed. The prototype of active arc suppression device was developed. The results of simulation and prototype experiment validate the effectiveness of the proposed method.

## 1 | INTRODUCTION

In the non-effective grounding distribution network, most of the power outage accidents are caused by single-line-to-ground (SLG) fault [1]. The intermittent grounding arc residual current and overvoltage caused by SLG faults endangers personal and equipment safety [2]. If fault isolation or removal measures are not taken in time, single-phase grounding faults may evolve into interphase short circuit faults, even cause substation deflagration, cable ditch fire and other dangerous accidents [3,4].

Peterson coil is a current arc suppression method which is the most common neutral grounding method for the medium voltage distribution network [5,6]. However, Peterson coil cannot compensate harmonic and active components of the fault current. It even weakens the influence of fault characteristics in complex distribution network, which makes it difficult for the protection device to accurately detect and select the faulty feeder [7,8].

In recent years, multiple voltage arc suppression methods are introduced. After the arc is extinguished, the fault point insulation medium recovery speed is faster than the fault voltage recovery speed, which can effectively prevent arc reignition. Thus, as long as the fault voltage is limited, effective arc extinguishing can be achieved. In [9,10], ground failover device for limiting intermittent arc grounding overvoltage is applied. The fault phase voltage is suppressed to zero by setting fault bypass grounding branch in the station to prevent the reignition of fault arc. But it is easy to misjudge the fault phase in the case of high resistance grounding fault, which may short-circuit the normal phase or interphase, causing tripping of outgoing circuit breaker.

Arc suppression based on power electronics devices with great flexibility has also drawn much attention in recent years. In [11,12], the controllable zero-sequence current generated by an active arc suppression device (ASD) is injected into the neutral point to achieve arc extinguishing effect. In literature [13,14], the zero-sequence voltage controlled by the ASD is adjusted to be the negative of the fault phase voltage, which constrains the recovery voltage at the fault point to zero, so as to achieve fault arc suppression. A hybrid flexible grounding system, which combines a large-capacity reactive power reactor with an

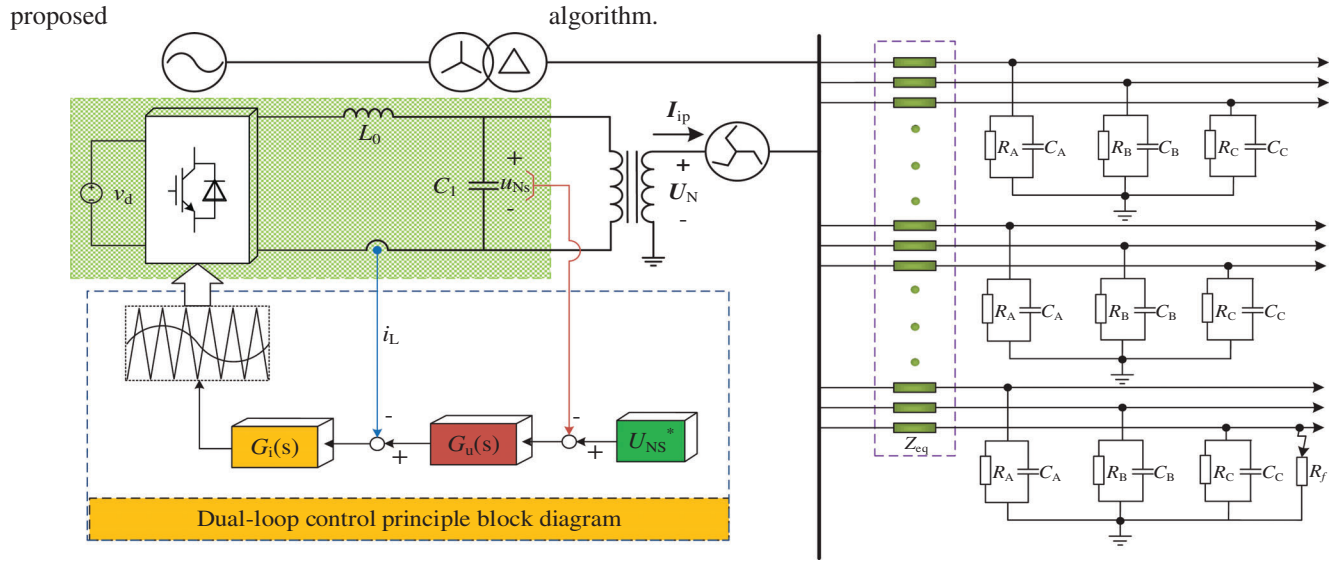


**FIGURE 1** Topology diagram of injection current arc suppression system

active power compensator for ground current compensation is mentioned in [15]. Most ASD methods can obtain satisfying grounding fault current compensation. However, in practical application, while considering line impedance, the arc suppression effect of the above methods is limited due to the line voltage drop between the fault point and the main line, especially, when the fault ground resistance is much smaller than the line impedance, which leads to inaccuracy of zero-sequence voltage control and results in large residual current of the grounding point.

In this paper, a novel voltage arc suppression method to accurately evaluate the line impedance is proposed. The injection zero-sequence voltage is theoretically analyzed by using line impedance, which achieves accurate grounding fault current compensation and reliable arc suppression effect. To accurately compensate residual current, a dual-loop voltage and current controller with accurate line impedance calculation is designed. The line currents before and after the SLG fault are sampled and calculated by difference to eliminate the influence of variational load current.

This paper is organized as follows. In Section 2, the novel principle of SLG fault arc suppression under complex distribution network is analyzed. An inverter-based dual-loop controller with line impedance is presented in Section 3. The proposed arc suppression method is verified in a typical 10 kV distribution network in MATLAB/Simulink in Section 4, and experimental results on a prototype are presented in Section 5 to verify the effectiveness of the proposed algorithm.

## 2 | PRINCIPLE OF ARC SUPPRESSION WITH CONSIDERATION OF LINE-IMPEDANCE EFFECT

Figure 1 is a simplified diagram of a 10 kv complex distribution network with an injected current arc suppression device. $\boldsymbol{E}_A$, $\boldsymbol{E}_B$ and $\boldsymbol{E}_C$ are the three-phase power supply voltages of complex distribution network, $\boldsymbol{U}_N$ is the neutral-to-ground voltage, $\boldsymbol{I}_{ip}$ is the injected current of the device. $R_f$ is the ground-fault resistance. $C_1$ and $L_0$ are the capacitance and inductance of the filter circuit, while $v_d$ is the external power supply voltage. $Z_{eq}$ is the line impedance from the fault point to the neutral point of the distribution network. The device consists of an external 380 V three-phase power supply, a single-phase inverter, a rectifier, and an isolation transformer, which are all listed in Table 1. The SLG fault is assumed to be phase C, the fault point is at the end of the line.

Figure 2 shows voltage vector diagrams of the SLG fault, where (a) does not take into account the existence of line impedance, and (b) considers the existence of the line impedance. $\boldsymbol{U}_A$, $\boldsymbol{U}_B$ and $\boldsymbol{U}_C$ are three-phase-to-ground bus voltages which are the same to three-phase power supply voltages $\boldsymbol{E}_A$, $\boldsymbol{E}_B$ and $\boldsymbol{E}_C$ before the SLG fault. $\boldsymbol{U}_f$ is the SLG fault-point-to-ground voltage and it is the same to the phase-to-ground voltage $\boldsymbol{U}_C$. $\boldsymbol{U}_{zeq}$ is the voltage drop of the line impedance. $\boldsymbol{U}_N$ is the neutral to ground voltage. As can be seen from Figure 2a, the SLG fault-point-to-ground voltage $\boldsymbol{U}_f$ is constrained to zero, when the amplitude of neutral voltage $\boldsymbol{U}_N$ is equal to the amplitude of power supply voltage $\boldsymbol{E}_C$, and the phase $\boldsymbol{U}_N$ is the opposite of the $\boldsymbol{E}_C$. However, as show in Figure 2b, while considering the existence of the line impedance, $\boldsymbol{U}_f$ and $\boldsymbol{U}_C$ are different. The $\boldsymbol{U}_f$ is constrained to zero, when the $\boldsymbol{U}_N$ is equal to $\boldsymbol{U}_{zeq} - \boldsymbol{E}_C$. Therefore, this paper proposes an active arc suppression strategy considering the existence of line impedance to achieve more accurate arc suppression.

In the proposed paper, the system is divided into two parts, that is, distribution network module and control module. The equivalent diagram of complex distribution network is shown in Figure 3. Notice that the three-phase-to-ground voltages are $\boldsymbol{U}_A$, $\boldsymbol{U}_B$ and $\boldsymbol{U}_C$, and the three-phase symmetric system is studied, leading to $R_A = R_B = R_C = R_0$, $C_A = C_B = C_C = C_0$. $C_0$

**TABLE 1** Distribution network and Asd variables

| Factor | Note |
|---|---|
| $U_A$, $U_B$, $U_C$ | Three-phase-to-ground bus voltages |
| $E_A$, $E_B$, $E_C$ | Three-phase power supply voltages |
| $I_A$, $I_B$, $I_C$ | Line-to-line currents |
| $R_A$, $R_B$, $R_C$ | Ground resistances |
| $C_A$, $C_B$, $C_C$ | Ground capacitances |
| $R_f$ | Ground fault resistance |
| $Z_{eq}$ | impedance of distribution network line |
| $I_{ip}$, $u_{NS}$ | Inverter output current, voltage |
| $v_d$ | DC voltage of the inverter |
| $L_0$, $C_1$ | Filter inductance, capacitance |
| $U_{Ns}^*$, $I^*$ | Dual-loop control voltage and current reference value |
| $U_N$ | Neutral-to-ground voltage |
| $E_0$ | Equivalent distribution network voltage source |
| $Z_s$ | Equivalent distribution network impedance |
| $N$ | Isolation transformer ratio |
| $G_{inv}$ | Inverter gain |
| $G_{PR}$, $G_{PI}$ | PR and PI controller coefficient |
| $f_0$ | Fundamental frequency |
| $U_{zeq}$ | Voltage drops on the line impedance |
| $U_f$ | SLG fault-point-to-ground voltage |
| $\Xi$ | The arc suppression efficiency |
| $I_{C0}$ | Phase C current simplified by difference calculation |
| $I_{C1}$, $I_{C2}$ | Phase C currents before and after the SLG fault |

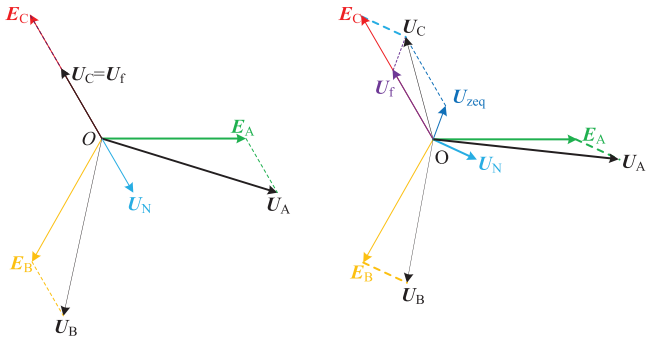


(a) *The existence of line impedance is not considered* (b) *Considering the existence of line impedance*

**FIGURE 2** Voltage vector diagrams of the SLG fault

and $R_0$ are phase to ground resistance and capacitance, respectively. According to Kirchhoff's law, the injection current $\boldsymbol{I}_{ip}$ can be obtained and is shown as (1):

$$\boldsymbol{I}_{ip} = \frac{\boldsymbol{U}_A + \boldsymbol{U}_B}{Z_{eq} + Z_0} + \frac{\boldsymbol{U}_C}{Z_{eq} + R_f // Z_0}, \tag{1}$$

where $Z_0 = R_0 // (1/j\omega C_0)$. Since three-phase-to-ground voltage is linked with the relationship of three-phase power supply and neutral-to-ground voltage, shown as follows, $\boldsymbol{U}_X = \boldsymbol{E}_X + \boldsymbol{U}_N$ (X = A, B or C), $\boldsymbol{E}_A + \boldsymbol{E}_B + \boldsymbol{E}_C = 0$. Thus, the injected current can be denoted as,

$$\mathbf{I}_{ip} = \mathbf{U}_C Z_{\sum 1} + 3\mathbf{U}_N \left(Z_{eq} + Z_0\right)^{-1}, \tag{2}$$

where $Z_{\sum 1} = (Z_{eq}+R_f)/(Z_0 Z_{eq}+R_f Z_{eq}+Z_0 R_f)\text{-}1/(Z_0+Z_{eq})$. Due to the line impedance, the faulty phase voltage cannot be treated as the fault point voltage $\boldsymbol{U}_f$, as the voltage on the line impedance $\boldsymbol{U}_{zeq}$ is satisfied with $\boldsymbol{U}_f + \boldsymbol{U}_{zeq} = \boldsymbol{U}_C$. Therefore, if $\boldsymbol{U}_f = 0$, then $\boldsymbol{U}_C = \boldsymbol{U}_{zeq}$; (2) can be replaced as,

$$\mathbf{I}_{ip} = \boldsymbol{U}_{zeq} Z_{\sum 1} + 3\mathbf{U}_N \left(Z_{eq} + Z_0\right)^{-1} \tag{3}$$

Notice that $\boldsymbol{U}_{zeq} = \boldsymbol{I}_C^* Z_{eq}$. Load current exists in the phase C line-to-line current, whose load capacity cannot be calculated in practice.

## 2.1 | Algorithm of the line impedance

According to (3), in order to obtain the reference of injected current $\boldsymbol{I}_{ip}$, the grounding impedance $Z_0$, the fault phase current $\boldsymbol{I}_C$ and the neutral-to-ground voltage $\boldsymbol{U}_N$ should be measured. Because the location of the fault point cannot be known in advance, and the ground fault resistance $R_f$ oscillates with the arc, the line impedance $Z_{eq}$ and $R_f$ cannot easily be measured or calculated. As the faulty phase current $\boldsymbol{I}_c$ includes load current which varies with time, methods should be adopted to eliminate the influence of the load current. The equivalent circuit diagram of a single feeder in the distribution network is shown in Figure 4.

To further simply the equivalent circuit in Figure 4, fault phase sequence network diagram is presented, as shown in Figure 5. In normal operation, there is only positive sequence in the system, so the total current $\boldsymbol{I}_{C1}$ of phase C can be obtained as:

$$\boldsymbol{I}_{C1} = \boldsymbol{E}_C / \left(Z_{eq} + Z_{load3}\right). \tag{4}$$

When SLG fault occurs, the Phase C equivalent circuit can be decomposed into three parts, the zero sequence, positive sequence, and negative sequence. Thus, the total current of phase C after SLG fault can be obtained as $\boldsymbol{I}_{C2}$,

$$\boldsymbol{I}_{C2} = \boldsymbol{E}_C / \left(Z_{eq} + Z_{load} // Z_0 // \left(3R_f + Z_0 + Z_{eq}/n + Z_{eq} // Z_{load} // Z_0\right)\right). \tag{5}$$

The instantaneous load before and after the fault can be regarded as constant. Therefore, by subtracting the phase C current before the fault from the current after the fault, the current $\boldsymbol{I}_{C0}$ using the differential method has eliminated the influence of the load current on the distribution network.

$$\boldsymbol{I}_{C0} = \boldsymbol{E}_C / \left(Z_{eq} + (Z_0 // R_f)\right). \tag{6}$$

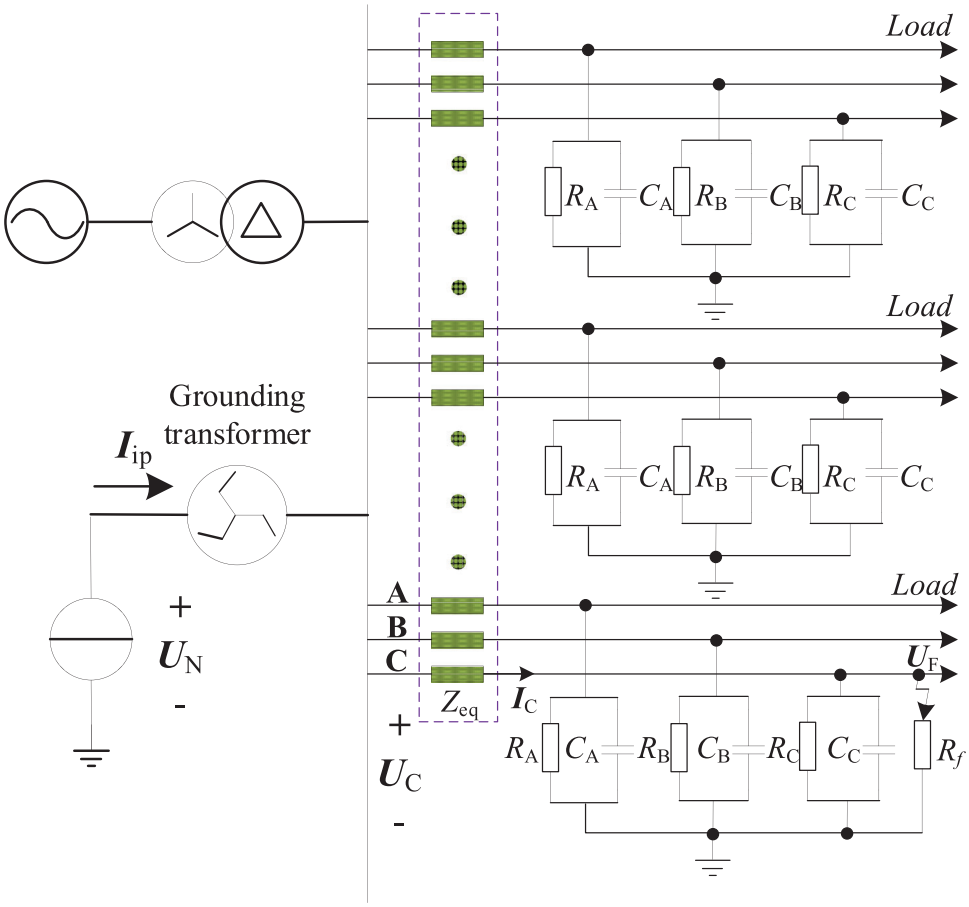


**FIGURE 3** Topology diagram of complex distribution network

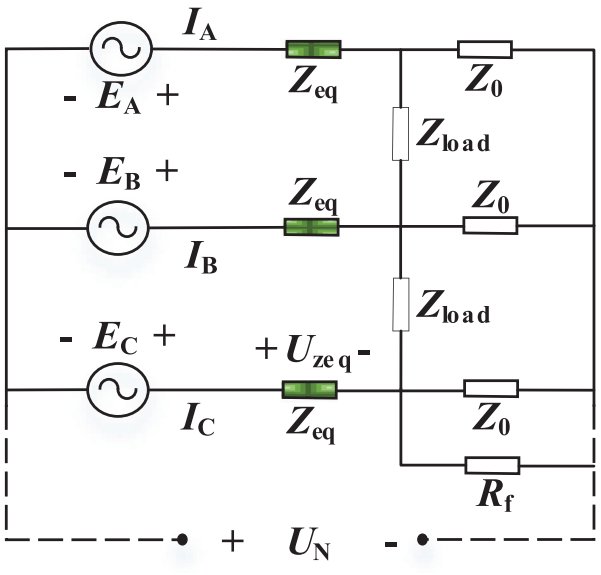


**FIGURE 4** Equivalent circuit diagram of distribution network

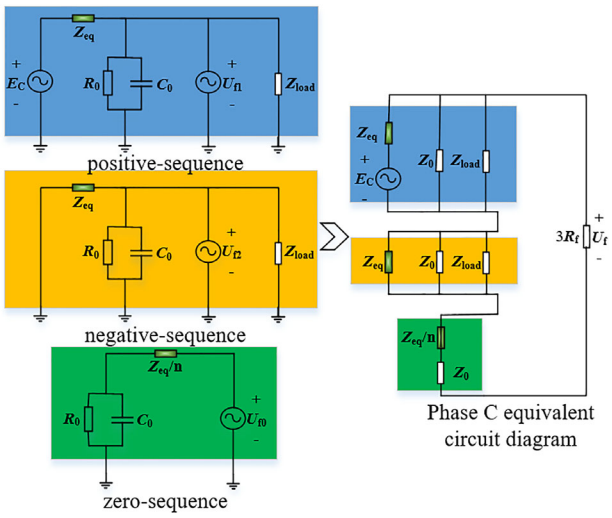


**FIGURE 5** Phase C equivalent sequence network diagram after SLG fault

Then, the phase C current ignoring the load current is $\boldsymbol{I}_{C0}$, and the simplified diagram of the equivalent circuit of the distribution network after SLG fault is shown in Figure 6.

According to Kirchhoff's current laws:

$$\begin{cases} \dfrac{\boldsymbol{U}_A + \boldsymbol{U}_B}{Z_{eq} + Z_0} + \dfrac{\boldsymbol{U}_C}{Z_{eq} + R_f // Z_0} = 0 \\ \dfrac{\mathbf{U}_A + \mathbf{U}_B - 2\mathbf{U}_{zeq}}{Z_0} + \dfrac{\mathbf{U}_C - \mathbf{U}_{zeq}}{Z_0 // R_f} = 0 \end{cases}. \tag{7}$$

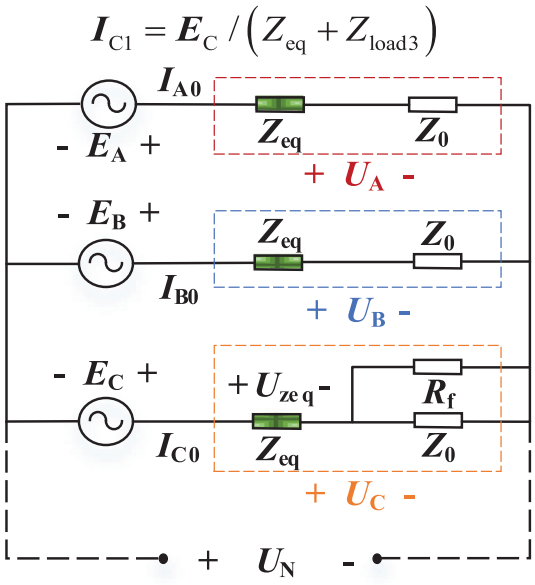


**FIGURE 6** Equivalent circuit diagram of simplified distribution network

Under the conditions of $\boldsymbol{U}_X = \boldsymbol{E}_X + \boldsymbol{U}_N$ (X = A, B or C) and $\boldsymbol{E}_A + \boldsymbol{E}_B + \boldsymbol{E}_C = 0$, (1) and (7) can be appropriately simplified as:

$$\begin{cases} 3\boldsymbol{U}_N \left(Z_0 Z_{eq} + Z_f Z_{eq} + Z_0 R_f\right) = -\boldsymbol{U}_C {Z_0}^2 \\ \boldsymbol{U}_C Z_0 + 3\boldsymbol{U}_N R_f = \boldsymbol{U}_{zeq} \left(Z_0 + 3R_f\right) \end{cases}. \tag{8}$$

There are unknown parameters $\boldsymbol{U}_{zeq}$, $Z_{eq}$ and $R_f$ in (8). $\boldsymbol{U}_{zeq} = \boldsymbol{I}_{C0} * Z_{eq}$ can be known from Figure 5. So, the formulation can be simplified to (9):

$$\begin{cases} \boldsymbol{I}_{C0} = \dfrac{\boldsymbol{U}_C Z_0 + 3\boldsymbol{U}_N R_f}{Z_{eq} \left(Z_0 + 3R_f\right)} \\ \boldsymbol{U}_N = \dfrac{-\boldsymbol{U}_C {Z_0}^2}{3\left(Z_0 Z_{eq} + Z_{eq} R_f + Z_0 R_f\right)} \end{cases}. \tag{9}$$

In (9), only $Z_{eq}$ and $R_f$ are unknown, and they can be figured out as,

$$Z_{eq} = -\frac{\boldsymbol{U}_N \boldsymbol{U}_C - 3{\boldsymbol{U}_N}^2 - \boldsymbol{U}_N Z_0 \boldsymbol{I}_{C0} + \boldsymbol{U}_C Z_0 \boldsymbol{I}_{C0}}{2Z_0 \boldsymbol{I}_{C0}}, \tag{10}$$

$$R_f = \frac{-Z_0 \left(3\boldsymbol{U}_N + Z_0 \boldsymbol{I}_{C0}\right)}{3\left(\boldsymbol{U}_N + Z_0 \boldsymbol{I}_{C0}\right)}. \tag{11}$$

Notice that the line impedance and ground fault resistance value above can be substituted into (3), further to get the accurate injection current value.

$$\mathbf{I}_{ip} = \boldsymbol{U}_{zeq} \left(\frac{Z_{eq} + R_f}{Z_0 Z_{eq} + R_f Z_{eq} + Z_0 R_f} + \frac{2}{Z_{eq} + Z_0}\right) - 3\boldsymbol{E}_C \left(Z_{eq} + Z_0\right)^{-1}, \tag{12}$$

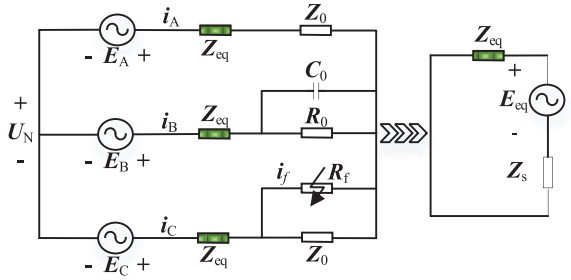


**FIGURE 7** Equivalent circuit of the distribution network

where $\boldsymbol{U}_{zeq} = -(\boldsymbol{U}_N \boldsymbol{U}_C - 3{\boldsymbol{U}_N}^2 - \boldsymbol{U}_N Z_0 \boldsymbol{I}_{C0} + \boldsymbol{U}_C Z_0 \boldsymbol{I}_{C0})/2\boldsymbol{U}_N$, and $\boldsymbol{U}_C = \boldsymbol{E}_C + \boldsymbol{U}_N$, $\boldsymbol{U}_f + \boldsymbol{U}_{zeq} = \boldsymbol{U}_C$, $\boldsymbol{U}_f = 0$. It is found that the injected current can be attained by substituting the line impedance $Z_{eq}$ and ground fault resistance $R_f$.

With the purpose of control reliability, the proposed paper intends to adopt a double closed-loop controller. According to Figure 6, the neutral-to-ground voltage $\boldsymbol{U}_N$ is equal to the difference between the phase C power supply voltage $\boldsymbol{E}_C$ and the voltage drops on the line impedance $\boldsymbol{U}_{zeq}$, which is shown in (13).

$$\boldsymbol{U}_N = \boldsymbol{U}_{zeq} - \boldsymbol{E}_C. \tag{13}$$

Finally, it is necessary to control the neutral-to-ground voltage to force the fault point-to-ground voltage to zero and complete the arc suppression.

The following chapter mainly introduces the application of dual-loop voltage control method to control the neutral point voltage in complex distribution network conditions.

## 3 | ACTIVE ARC SUPPRESSION CONTROL

The distribution network is a 10 kV power system. As the bolted ground fault rarely happens, the ground-fault resistance $R_f$ is chosen to be 10 Ω to 10 kΩ in case study [14]. Thus, the power stage of the distribution network is in fundamental frequency, in which the distribution network can be treated as series connected voltage source $\boldsymbol{E}_0$ and zero-sequence impedance of the distribution network $Z_0$, expressed in [15], where $R_0$, $C_0$ are set as the symmetric phase-to-ground parameters of three-phase, $Z_{eq}$ is the line impedance.

Figure 7 is a simplified diagram of the equivalent circuit of the distribution network. Then, (14) and (15) can be obtained by applying Thevenin equivalent transformation.

$$\boldsymbol{E}_0 = -\frac{\mathbf{E}_C}{N} \frac{R_0}{3sR_f R_0 C_0 + 3R_f + R_0}, \tag{14}$$

$$Z_s = \frac{R_0 R_f}{N^2 \left(3sR_f R_0 C_0 + 3R_f + R_0\right)}. \tag{15}$$

The expressions of $\boldsymbol{E}_0$ and $Z_s$ can be obtained by applying the applied voltage source method. Then can see that a complex distribution network is reduced to a series of voltage sources and resistors.

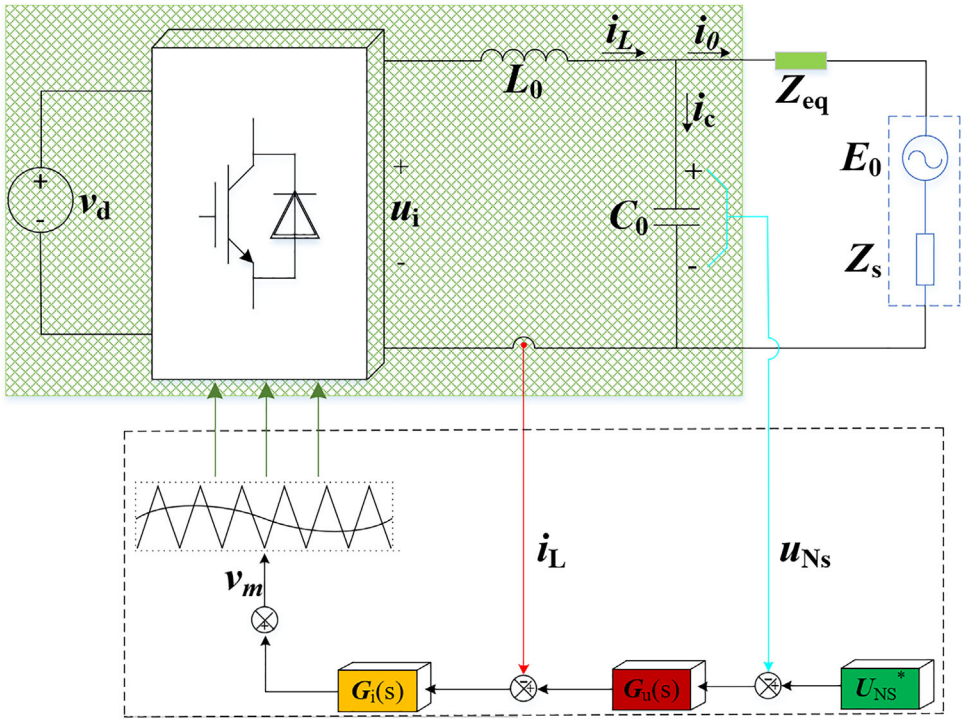


**FIGURE 8** Active arc suppression system with dual-loop control method

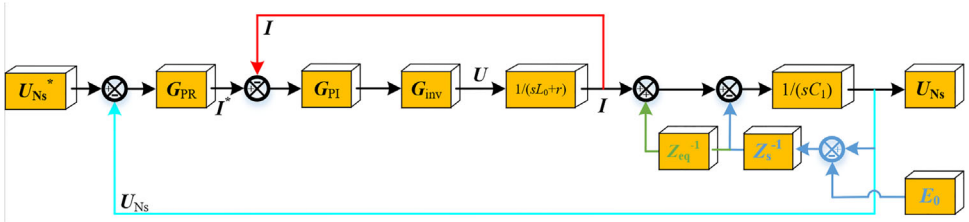


**FIGURE 9** Block diagram of the dual-loop control method

It can be seen from (3) that the injected current is determined by the network's parameters, such as ground admittance and line impedance of the line. In order to realize the control of zero-sequence voltage, the closed-loop control technology of power electronic equipment is adopted [16,17]. The amplitude and phase of the injected current are feedback controlled, and the fault phase voltage is forced to be zero, to achieve the purpose of voltage suppression [18,19]. The structure of the control part is shown in Figure 8.

The proposed paper adopts a double closed loop control system, including an inner current loop and an outer voltage loop. The voltage outer ring provides a reference voltage $\boldsymbol{U}_{\mathbf{Ns}}{}^*$ to the current inner ring, which provides a reference current $\boldsymbol{I}^*$ to the voltage outer ring. Then, through the voltage outer ring, the neutral-to-ground voltage $\boldsymbol{U}_{\mathbf{N}}$ can be controlled. The dual-loop control block diagram is as follows in the Figure 8, where PI controller is used for the inner current loop, PR controller is used for the outer voltage loop, and the inner and outer loops are in series.

In the Figure 9, $\boldsymbol{U}_{\mathbf{Ns}}{}^*$, $\boldsymbol{I}^*$, $\boldsymbol{I}$ and $\boldsymbol{U}$ are the negative number of fault phase voltage, output current reference value, output current detection value and inverter output voltage, respectively. $G_{PR}$, $G_{PI}$ and $G_{inv}$ are the transfer functions of PR controller, PI controller and inverter respectively. $1/(sL_0+r)$ is the simplified transfer function of the filter module, and $\boldsymbol{E}_0$ and $Z_0$ are the equivalent voltage and impedance of the distribution network after Thevenin equivalent change, respectively. By using the transfer function block diagram, we can simplify it again and replace a feedback function with a forward channel transfer function, which can greatly simplify the analysis processes. The diagram is as follows in the Figure 10. New parameters are obtained after simplification:

$$G_{kb} = \frac{sC_1\left(Z_s + Z_{eq}\right)}{1 + sC_1\left(Z_s + Z_{eq}\right)} = \frac{sC_1R_0\left(R_f + Z_{eq} + Z_s\right)}{sR_0\left(R_f + Z_{eq}\right)\left(3N^2C_0 + C_1\right) + \left(3Z_{eq} + 3Z_s + 3R_f + R_0\right)N^2}. \tag{16}$$

Figures 11 and 12 are the Bode diagrams of the transfer function $G_{kb}$ when the fault ground resistance changes/unchanged

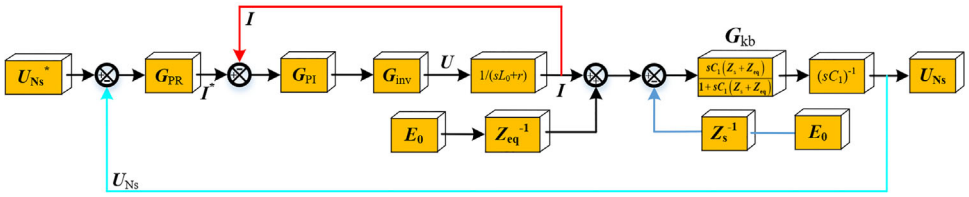


**FIGURE 10** Block diagram of simplified dual-loop control method

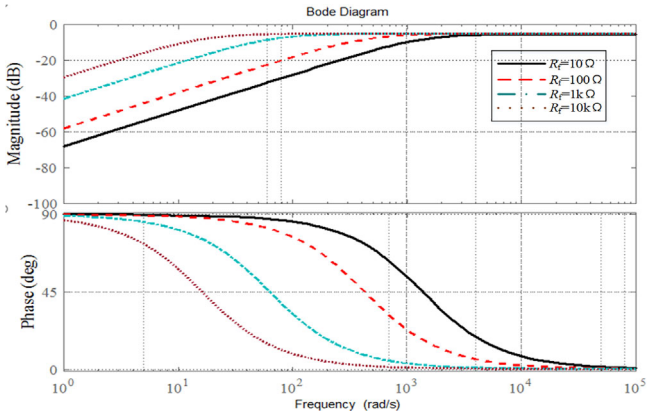


**FIGURE 11** Bode diagram of $G_{kb}$ when $R_f$ varies and $Z_{eq} = 30 + j\ \Omega$

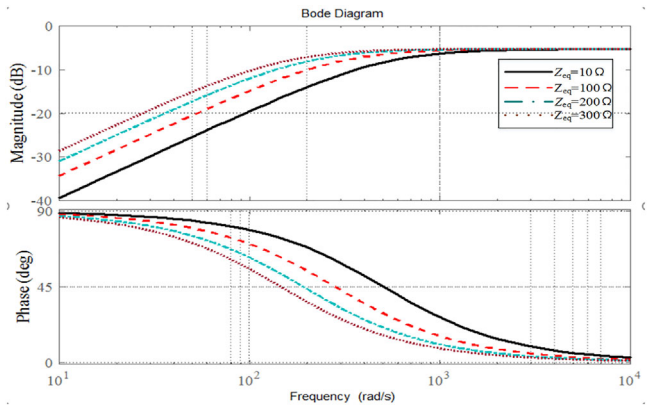


**FIGURE 12** Bode diagram of $G_{kb}$ when $Z_{eq}$ varies and $R_f = 100\ \Omega$

and the line impedance is fixed. It can be clearly seen in Figure 11 that it is in low frequency band, and the gain obtained by high impedance grounding is greater than that by low impedance grounding. While in Figure 12 the gain of low frequency band increases with the increase of $Z_{eq}$, and the anti-interference ability is poor under heavy load.

The output current of the current inner loop is controlled by the active arc suppression device and the output current of the voltage outer loop is taken as the reference value. The high precision real-time control of the output current is realized by the PI controller. The transfer function of the current inner loop is,

$$G_{cp} = \frac{G_{PI}G_{inv}}{SL_0 + r + G_{PI}G_{inv}}. \tag{17}$$

Parameter in the formula, $G_{PI} = K_p(1+K_i/s)$, $K_p$ and $K_i$ are the proportional coefficient and integral coefficient of PI controller respectively. The $G_{inv} = K_{inv}$, $K_{inv}$ is the proportional coefficient of the inverter.

The neutral-to-ground voltage $\boldsymbol{U}_N$ is the control target of the dual-loop. In order to suppress the ground fault voltage to zero, the reference voltage should be equal to the difference between the voltage on the line impedance and the phase C power supply voltage. The outer ring controller compares the difference between the reference value and the neutral point voltage in real time, and gets the reference value of the inner current through PI. So that the neutral point voltage approximates the difference between the voltage on the line impedance and the phase C power supply voltage, and then the fault point voltage is limited to zero. The transfer function of the $\boldsymbol{U}_{NS}$ is:

$$\boldsymbol{U}_{NS} = G_1\boldsymbol{U}_{NS}^* + G_2\boldsymbol{E}_0. \tag{18}$$

According to the transfer function of Figure 9, using the characteristics and principle of the system's multi-input single output, $G_1$ and $G_2$ can be obtained respectively.

$$G_1 = \frac{G_{PR}G_{cp}G_{kb}}{SC_1 + G_{kb}G_{PR}G_{cp}}, \tag{19}$$

$$G_2 = \frac{G_{kb}\left(Z_{eq} + Z_s\right)^{-1}}{SC_1 + G_{kb}G_{PR}G_{cp}}, \tag{20}$$

where $G_{PR} = k_p + 2k_r\omega_c s/(s^2+2\omega_c s+\omega^2)$, $K_p$ and $K_r$ are the proportional coefficient and resonance coefficient of PR controller, respectively, and $\omega_c$ is the resonant cutoff frequency.

As the voltage detection method only provides the reference voltage instruction for the outer voltage loop, and has no influence on the controller of the inner current loop, the proposed voltage detection method does not affect the output current THD. The current THD limit can be realized by reasonable selection of output filter inductor, switching frequency and current inner loop control method [21]. The efficiency can be improved by selecting switching frequency and reducing parasitic resistance parameters [22].

Therefore, the arc suppression process of SLG fault in distribution network is shown in Figure 13. First, three-phase voltage and acquisition of the neutral point voltage when the neutral point voltage change is more than 15% of the phase voltage, for ground-fault recognition, The fault phase is selected by comparing the amplitude and phase changes of three-phase-to-ground

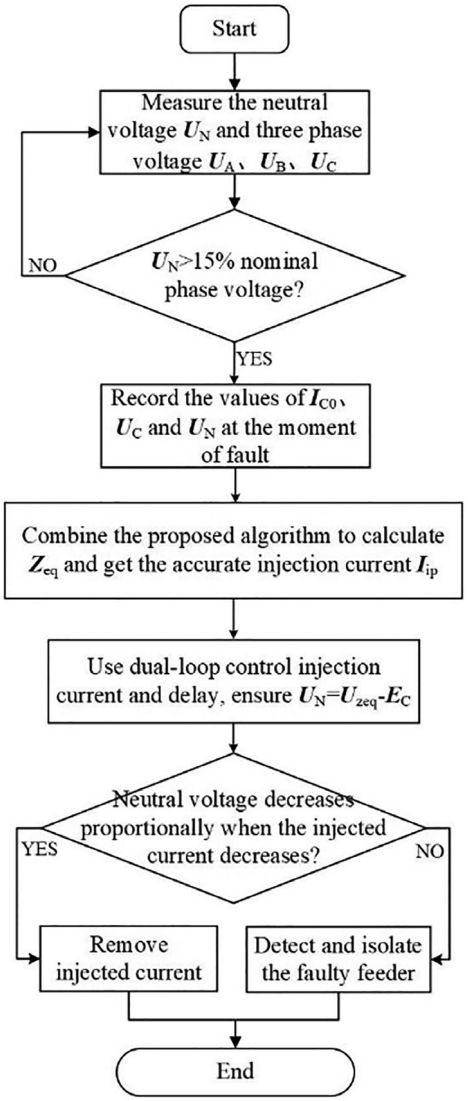


**FIGURE 13** Flowchart of active current suppression method

voltage before and after fault occurrence [20]. By recording the values of relevant parameters in the distribution network before and after the fault, the algorithm proposed in this paper is used to calculate the line impedance, and the voltage drop $\boldsymbol{U}$ on the line impedance is obtained. The reference voltage is determined by the voltage drop on the line impedance minus the faulty phase voltage, and the neutral point voltage is controlled through the output of the dual closed-loop controller. Hence, ground-fault voltage and current at the fault point of the complex distribution network are set to zero, to achieve the purpose of arc suppression. Finally, the injected current is removed when the fault is eliminated.

## 4 | SIMULATION

A 10 kV distribution network simulation model was established in MATLAB. In addition, two states are simulated in the control algorithm. Both considers the line impedance of complex distribution network, but one is adapted conventional ASD method [12], and the other applies the proposed algorithm. Their arc suppression effects are simulated in the case of high resistance and low resistance. The parameters of the distribution network and controller are listed in Table 2.

**TABLE 2** Parameters for case study

| | Parameters | Values |
|---|---|---|
| Distribution network | Damping ratio $d$ | 0.08 |
| | Leakage resistance $R_0$ | 12.7kΩ |
| | Nominal distributed capacitance $C_0$ | 8.36uF |
| | Fundamental frequency $f_0$ | 50 Hz |
| | Line-to-neutral voltage $E_x$ | 5.77kv |
| | Line-to-line voltage $U_X$ | 10kv |
| | Ground fault resistance $R_F$ | 0.01-10kΩ |
| Active ASD | Isolation transformer ratio $N$ | $10.5/\sqrt{3}$ : 0.3 |
| | Isolation transformer capacity | 100kVA |
| | Isolation transformer leakage inductance (low voltage side) | 0.01mH |
| | Filter inductance $L_0$ | 0.5mH |
| | Filter inductor ESR $r$ | 0.2Ω |
| | Filter capacitance $C_P$ | 10uF |
| | Inverter gain $G_{inv}$ | 600 |
| | Dc voltage $v_d$ | 600V |

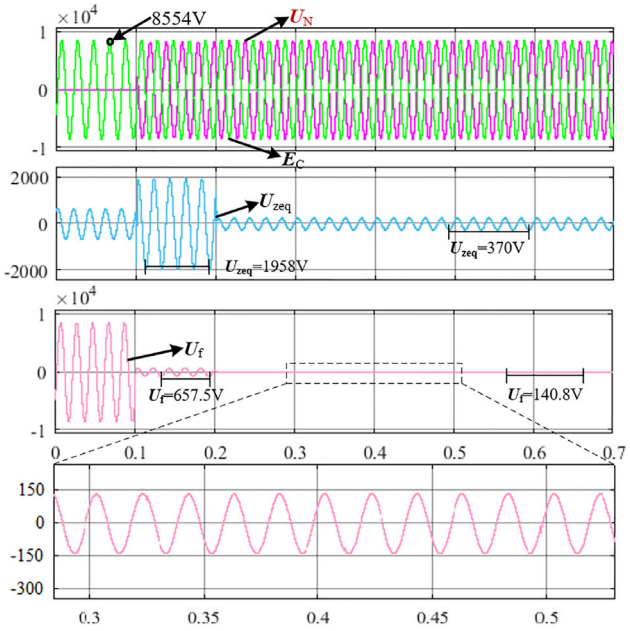


**FIGURE 14** Simulation waveforms of conventional method when $R_f$ = 10 Ω and $Z_{eq}$ = 30+0.01 jΩ

Figure 14 shows the simulation results of the proposed method when $R_f$ = 10Ω and $Z_{eq}$ = 30+0.01 jΩ. At 0.1 s, the ground-fault resistance is connected. And the arc suppression device is turned on at 0.2s, at this time, the voltage of the control neutral-to-ground $\boldsymbol{U}_N$ is -$\boldsymbol{E}_C$. After 0.3 s, the SLG fault-point-

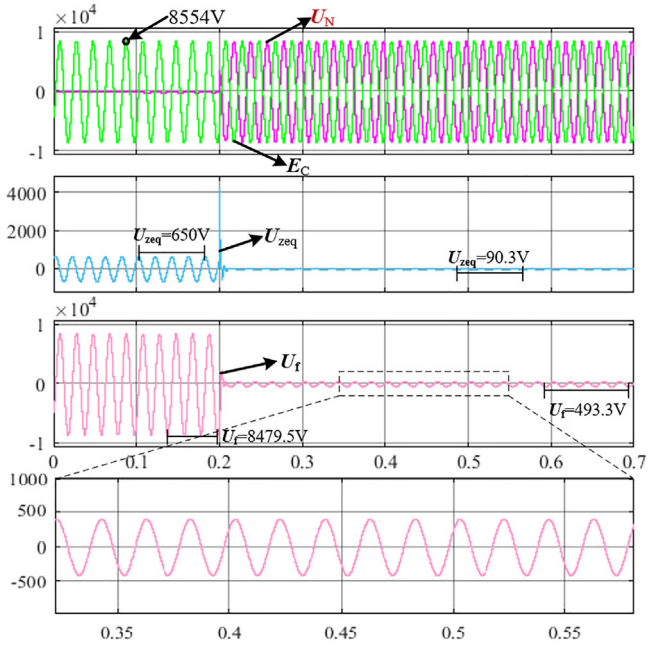


**FIGURE 15** Simulation waveforms of conventional method when $R_f = 10\ \text{k}\Omega$ and $Z_{eq} = 30+0.01\ \text{j}\Omega$

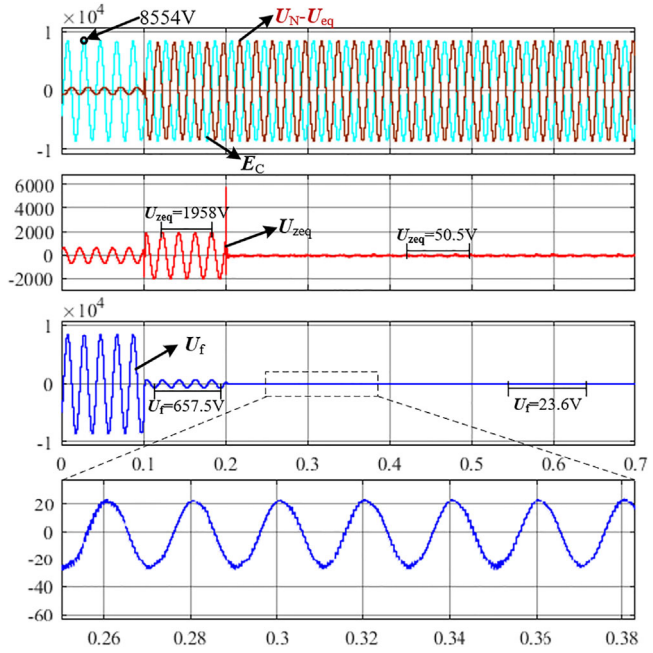


**FIGURE 16** Simulation waveforms of the proposed method when $R_f = 10\ \Omega$ and $Z_{eq} = 30+0.01\ \text{j}\Omega$

to-ground voltage $\boldsymbol{U}_\text{f}$ decreases from 657.5 V to 140.8 V. The arc suppression efficiency is

$$\xi = \frac{(657.5\text{V} - 140.8\text{V})}{657.5\text{V}} \times 100\% \approx 78.6\%.$$

Figure 15 shows the simulation results of the proposed method when $R_f = 10\text{k}\Omega$ and $Z_{eq} = 30+0.01\text{j}\Omega$. At 0.1 s, the ground-fault resistance is connected, and the arc suppression device is turned on at 0.2 s. After 0.3 s, the SLG fault-point-to-ground voltage $\boldsymbol{U}_\text{f}$ decreases from 8479.5 V to 493.3 V. The arc suppression efficiency is

$$\xi = \frac{(8479.5\text{V} - 493.3\text{V})}{8479.5\text{V}} \times 100\% \approx 94.2\%.$$

Figure 16 shows the simulation results of the proposed method when $R_f = 10\ \Omega$ and $Z_{eq} = 30+0.01\ \text{j}\Omega$. The ground-fault resistance is connected to the distribution network at 0.1 s. And the ASD is activated at 0.2 s, at this time, the voltage of the control neutral-to-ground $\boldsymbol{U}_\text{N}$ is $\boldsymbol{U}_{\text{zeq}}$-$\boldsymbol{E}_\text{C}$. After 0.3 s, the SLG fault-point-to-ground voltage $\boldsymbol{U}_\text{f}$ decreases from 657.5 V to 23.6 V. The arc suppression efficiency is

$$\xi = \frac{657.5\text{V} - 23.6\text{V}}{657.5\text{V}} \times 100\% \approx 96.4\%.$$

Figure 17 shows the simulation results of the proposed method when $R_f = 10\ \text{k}\Omega$ and $Z_{eq} = 30+0.01\ \text{j}\Omega$. Ground-fault resistance is connected to the distribution network at 0.1 s, and the ASD is activated at 0.2 s. After 0.3 s, the SLG fault-point-to-ground voltage $\boldsymbol{U}_\text{f}$ decreases from 8479.5 V to 63.3 V. The arc

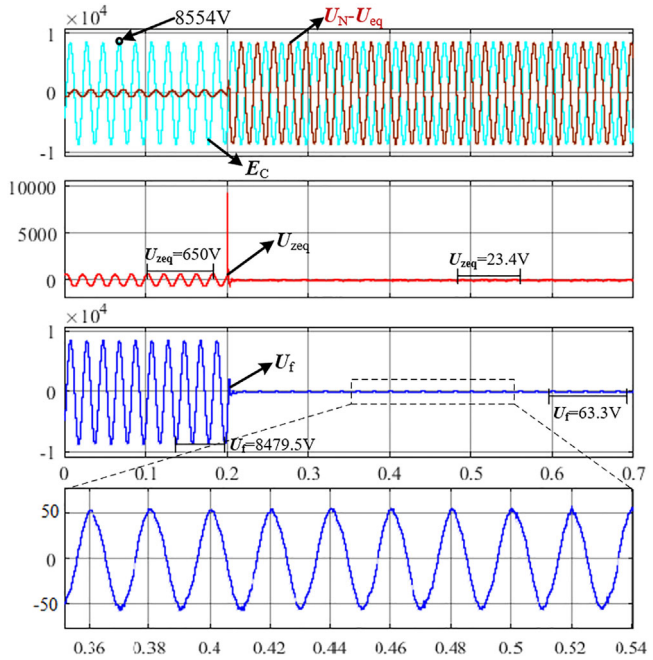


**FIGURE 17** Simulation waveforms of the proposed method when $R_f = 10\ \text{k}\Omega$ and $Z_{eq} = 30+0.01\ \text{j}\Omega$

suppression efficiency is

$$\xi = \frac{8479.5\text{V} - 63.3\text{V}}{8479.5\text{V}} \times 100\% \approx 99.3\%.$$

Combined with the above two states, different ground fault resistance waveforms are simulated. It is found that the

**TABLE 3** Simulation data in a variety of complex distribution network

| $R_f$ | $Z_{eq}$ | $\xi$ *of* Conventional ASD | $\xi$ *of* Proposed ASD |
|---|---|---|---|
| 10Ω | 30+0.01j | 78.6% | 96.4% |
| 1kΩ | 30+0.01j | 83.3% | 98.6% |
| 10kΩ | 30+0.01j | 94.2% | 99.3% |
| 10Ω | 40+0.1jΩ | 87.4% | 96.3% |
| 1kΩ | 40+0.1jΩ | 91.3% | 98.7% |
| 10kΩ | 40+0.1jΩ | 94.3% | 99.7% |
| 10Ω | 50+0.5jΩ | 80.2% | 96.2% |
| 1kΩ | 50+0.5jΩ | 82.6% | 97.9% |
| 10kΩ | 50+0.5jΩ | 85.0% | 98.8% |

**TABLE 4** experimental parameters

| Coefficients | Values | Units |
|---|---|---|
| Resonant cutoff frequency $\omega_c$ | 3.14 | rad/s |
| Line impedance $Z_{eq}$ | 30+0.01j | Ω |
| Grounding fault resistance $R_f$ | 10,10000 | Ω |
| Outer-loop Resonant ratio $K_p$ | 5 | – |
| Outer-loop Resonant ratio $K_i$ | 23 | – |
| Outer-loop Resonant ratio $K_r$ | 1 | – |
| Nominal phase-to-ground resistance $R_0$ | 200 | Ω |
| Nominal phase-to-ground capacitance $C_0$ | 200 | uF |
| Line-to-neutral voltage $E_x$ | 220 | V |
| Isolation transformer ratio $N$ | 1:1 | – |
| Isolation transformer capacity | 20 | kVA |
| Switching frequency $f_{sw}$ | 10 | kHz |

conventional method is not satisfactory compared with the proposed ASD method when the line impedance is considered, and after arc suppression, there is still a large residual current in the actual line. On the contrary, under the same conditions, the proposed method has better effect, faster response speed, higher control accuracy and more reliable arc suppression. Found that under same conditions, when the line impedance value is larger, the conventional ASD method's effect is worse, and the proposed ASD method with the new algorithm has more obvious advantages. Especially when the line impedance is much larger than the ground fault resistance, the comparison effect is more notable.

Table 3 shows the data comparison of simulation between the conventional arc suppression method and the arc suppression method under various line impedance conditions.

## 5 | EXPERIMENT

In order to verify the arc suppression effect of SLG fault in complex distribution network, a corresponding physical simulation was also carried out in this paper. Figure 18 is the physical simulation system. The parameters of the distribution network and the ASD are the same as the simulation in MATLAB/Simulink in Section IV. So, the experiment parameter values are shown in Table 4, and the experiment results are shown as follows.

As shown in Figure 18, 10 kV power supply system is formed by 380 V power supply, a self-coupling transformer and a boosting transformer. The main circuit of the active device consist of a three-phase control rectifier and single-phase full bridge inverter with an LC type filter. The rated voltage and current of the IGBT modules of the inverter is 1, 200 V and 400 A, respectively.

The digital signal controller TMS320F28335 from Texas Instruments is used as the controller for power electronic switches. The other parts of the experimental system are the

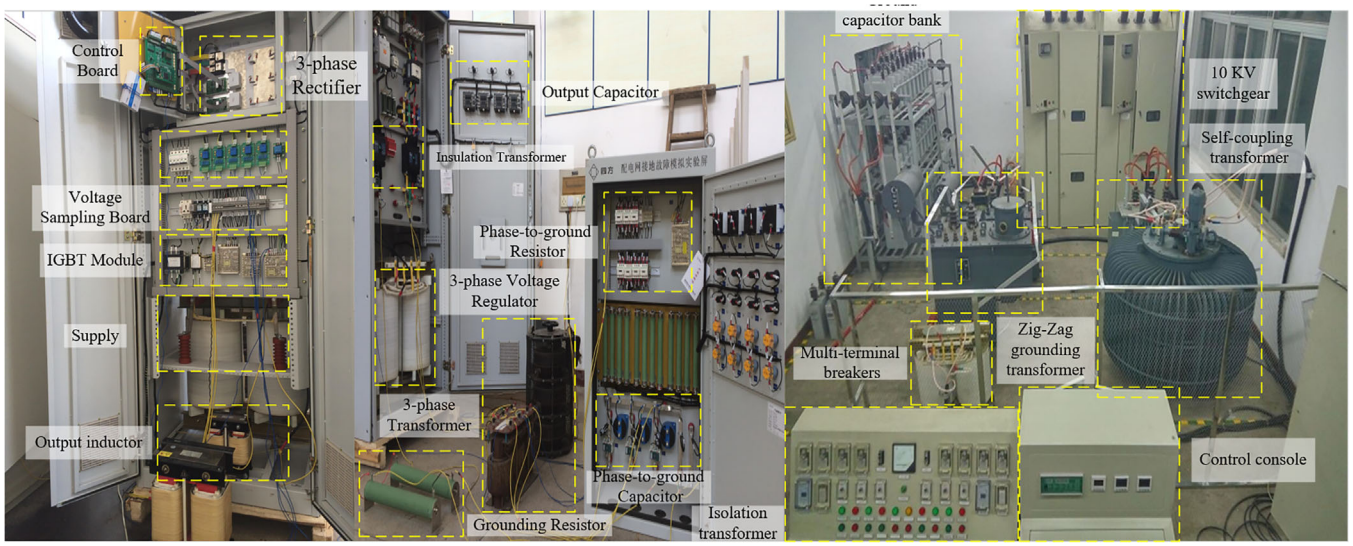


**FIGURE 18** Experimental platform for flexible grounding system of distribution network

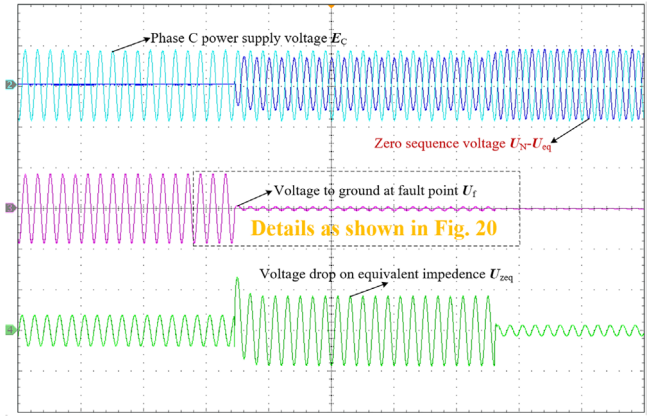


**FIGURE 19** Experiment result when Rf = 10 Ω and Zeq = 30+0.01j Ω.
CH1: Power supply voltage (10000 V/div, t:0.1 s/div)
CH2: Zero sequence voltage (10000 V/div, t:0.1 s/div)
CH3: Voltage to ground at fault point (1000 V/div, t:0.1 s/div)
CH4: Voltage drop on line impendence (5000 V/div, t:0.1 /div)

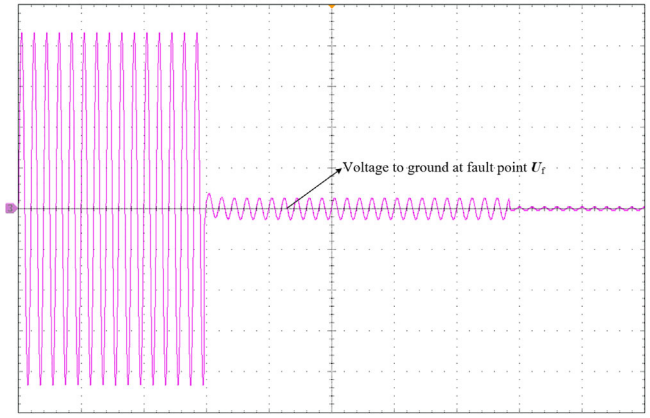


**FIGURE 20** Experiment result when $R_f$ = 10 kΩ and Zeq = 30+0.01 jΩ.
(CH3: Voltage to ground at fault point (2000 V/div, t:0.1 s/div))

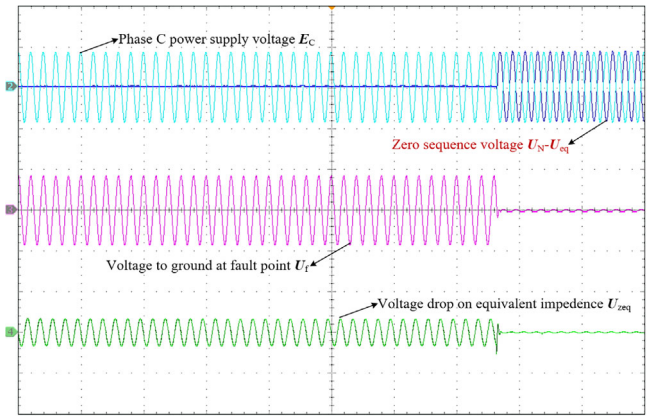


**FIGURE 21** Experiment result when $R_f$ = 10 kΩ and Zeq = 30+0.01 jΩ.
CH1: Power supply voltage (10000 V/div, t:0.1 s/div)
CH2: Zero sequence voltage (10000 V/div, t:0.1 s/div)
CH3: Voltage to ground at fault point (10000 V/div, t:0.1 s/div)
CH4: Voltage drop on line impendence (2000 V/div, t:0. 1s/div)

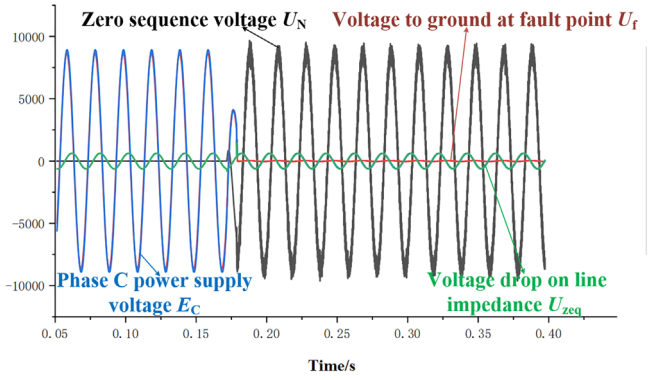


**FIGURE 22** Analysis of equation ($U_N = U_{zeq}$-$E_C$) from Experiment data of the existing oscilloscope, additional sensors are added to capture the accurate experiment results

same as Figure 1. The test scenarios in Section IV are duplicated in this experiment for comparison.

As shown in Figure 19, at the moment of fault occurrence, the voltage to earth at the fault point rises sharply and the neutral point generates high voltage. After 0.2 s, the arc suppression device is connected, since the ground resistance value is small and the line impedance is large, the resistance to the ground at the fault point decreases sharply. As shown in Figure 20, the voltage at the fault point drops from 678.4 V to 28.7 V. The effect of arc suppression is 95.8%. When the fault resistance is set as 10kΩ, the voltage measurements are out of the range

Therefore, the experiment results are given in Figure 21. The faulty phase voltage is reduced to 103 V. Arc suppression effect reached 98.8%. In Figure 20, fast dynamic response can be observed from the faulty point voltage. Thus, the proposed ASD method is effective in complex distribution network.

As we record the information from practical situation, the relationship among phase C supply voltage, voltage to ground at fault point, zero-sequence voltage and line impedance voltage can be obtained in Figure 22, where the (13) can be proved as accurate if fault occurs at phase C. Therefore, with the consideration of the line impedance, the distribution network can still be able to suppress the fault arc, if applying the proposed method.

## 6 | CONCLUSION

The proposed arc suppression method eliminates the influence of the line impedance voltage drop on the existing arc suppression methods and achieves more efficient voltage suppression at SLG fault points. The contribution and limitation of the paper is concluded as follows,

1. A Novel algorithm is presented to calculate the line impedance with the differential method, so that the influence of load current can be eliminated.

2. With the assistance of a novel algorithm for line impedance calculation based on three-phase-to-ground currents and the presented voltage control method, the injected current of the device can be calculated by the neutral voltage and fault phase voltage, which can achieve much better performance than the traditional current control method.
3. Compared with the conventional active voltage type arc suppression method, the proposed method has more accurate arc suppression effect under the actual complex distribution networks.
4. The stability analysis indicates that the stability of the proposed control system could be easily guaranteed. The developed prototype is set up to operate in a real, complex non-effectively earthed distribution system.
5. As the active voltage arc suppression device is an important primary equipment, further studies need to focus on the construction of regulations, test, and engineering verification in the future to popularize and apply the proposed ASD in power system.

## ACKNOWLEDGEMENTS

This work was supported in part by the National Natural Science Foundation of China under Award 51877011 and 52077010, and in part by Training Program for Excellent Young Innovators of Changsha under Award kq2009011.

## CONFLICT OF INTEREST

None of the authors have a conflict of interest to disclose.

## PERMISSION TO REPRODUCE MATERIALS FROM OTHER SOURCES

None

## DATA AVAILABILITY STATEMENT

The data that support the findings of this study are available from the corresponding author upon reasonable request.

## ORCID

*Wen Wang* https://orcid.org/0000-0003-1867-0937

## REFERENCES

1. Vaziri, M., Smith, D.R.: Grounding of primary system for LV networks. IEEE Trans. Power Del. 31(2), 419–427 (2016)
2. Ing, K.G., Jamian, J.J., Mokhlis, H., et al.: Optimum distribution network operation considering distributed generation mode of operations and safety margin[J]. IET Renewable Power Gener. 10(8), 1049–1058 (2016)
3. Cong, Z., Liu, Y., Fang, J., et al.: Root-cause identification of single line-to-ground fault in urban small current grounding systems based on correlation dimension and average resistance[J]. IEEE Trans. Power Delivery 35(4), 1834–1843 (2019)
4. Sörensen, S., Nielsen, H., Jørgensen, H.J.: Influence of harmonic voltages on single line to ground faults in distribution networks with isolated neutral or resonant earthing[C]. In: CIRED 2005-18th International Conference and Exhibition on Electricity Distribution, pp. 1–4. IET, Stevenage (2005)
5. Zeng, X., Xu, Y., Wang, Y.: Some novel techniques for insulation parameters measurement and Petersen-coil control in distribution systems. IEEE Trans. Ind. Electron. 57(4), 1445–1451 (2010)
6. Ran, J., Yang, Q., Chen, S., He, L.: An improved scheme for flexible grounding fault suppression in distribution system based on IGBT. Proceedings of IEEE International Conference on High Voltage Engineering and Application (ICHVE), pp. 1–4. IEEE, Piscataway (2018)
7. Huang, C., Tang, T., Jiang, Y., Hua, L., Hong, C.: Faulty feeder detection by adjusting the compensation degree of arc-suppression coil for distribution network. IET Gener. Transmiss. Distrib. 12(4), 807–814 (2018)
8. Zeng, X.J., Wang, Y.Y., Li, J., Xiong, T.T.: Novel principle of faults arc suppressioning & feeder protection based on flexible grounding control for distribution networks. Proc. CSEE 32, 0258–8013 (2012)
9. Feng, S., Zheng, L., Lie, J., et al.: Research on arc-grounding overvoltage in the 10 kV distribution system. Energy Procedia 16, 1785–1791 (2012)
10. Wang, F., Gao, H., Sun, Y., et al.: Arc grounding model and simulation in non-effectively grounded system[C]. In: 2015 5th International Conference on Electric Utility Deregulation and Restructuring and Power Technologies (DRPT), pp. 358–362. IEEE, Piscataway (2015)
11. Yuan, X., Li, Y., Wang, C.: Objective optimisation for multilevel neutral-point-clamped converters with zero-sequence signal control. IET Power Electron. 3(5), 755–763 (2010)
12. Wang, W., Zeng, X., Yan, L., Xu, X., Guerrero, J.M.: Principle and control design of active ground-fault arc suppression device for full compensation of ground current. IEEE Trans. Ind. Electron. 64(6), 4561–4570 (2017)
13. Zhang, J., Hu, L., Xu, S., et al.: Fault-tolerant compensation control for T-type three-level inverter with zero-sequence voltage injection[J]. IET Power Electron. 12(14), 3774–3781 (2019)
14. Wang, W., Yan, L., Zeng, X., Fan, B., Guerrero, J.M.: Principle and design of a single-phase inverter-based grounding system for neutral-to-ground voltage compensation in distribution networks. IEEE Trans. Ind. Electron. 64(2), 1204–1213 (2017)
15. Fan, B., Yao, G., et al.: Principle and control design of a novel hybrid arc suppression device in distribution networks. IEEE Trans. Ind. Electron. 69(1), 41–51 (2022). https://doi.org/10.1109/TIE.2021.3050390
16. Fang, X., Tian, Z., Li, H., et al.: Current closed-loop control and field orientation analysis of an induction motor in six-step operation for railway applications. IET Power Electron. 12(6), 1462–1469 (2019)
17. Rathore, A.K., Bhat, A.K.S., Nandi, S., et al.: Small signal analysis and closed loop control design of active-clamped zero-voltage switched two inductor current-fed isolated DC–DC converter. IET Power Electron. 4(1), 51–62 (2011)
18. Panfilov, D., Husev, O., Blaabjerg, F., et al.: Comparison of three-phase three-level voltage source inverter with intermediate dc–dc boost converter and quasi-Z-source inverter. IET Power Electron. 9(6), 1238–1248 (2016)
19. Paramasivan, M., Paulraj, M.M., Balasubramanian, S.: Assorted carrier-variable frequency-random PWM scheme for voltage source inverter. IET Power Electron. 10(14), 1993–2001 (2017)
20. Fan, B., Yao, G., Wang, W., Ma, H., et al.: Faulty phase recognition method based on phase-to-ground voltages variation for neutral ungrounded distribution networks. Electr. Power Syst. Res. 190, 106848 (2021), ISSN 0378-7796
21. Hu, Y., Du, Y., Xiao, W., et al.: DC-link voltage control strategy for reducing capacitance and total harmonic distortion in single-phase grid-connected photovoltaic inverters[J]. IET Power Electron. 8(8), 1386–1393 (2015)
22. Wu, F., Li, B., Duan, J.: Calculation of switching loss and current total harmonic distortion of cascaded multilevel grid-connected inverter and Europe efficiency enhancement considering variation of DC source power[J]. IET Power Electron. 9(2), 336–343 (2016)

**How to cite this article:** Fan, B., Ma, H., Wang, W., Yao, G., Li, Q., Zeng, X., Guerrero, J.M.: Active arc suppression device based on voltage-source convertor with consideration of line impedance in distribution networks. IET Power Electron. 2021;14:2585–2596. https://doi.org/10.1049/pel2.12203